Viscoelastic deformation for a clustered earthquake cycle

Brendan J. Meade[1] and Bradford H. Hager

Department of Earth, Atmospheric and Planetary Sciences, Massachusetts Institute of Technology, Cambridge, Massachusetts, USA

Received 3 February 2004; revised 8 April 2004; accepted 22 April 2004; published 25 May 2004.

[1] The clustering of earthquakes in time on the same fault affects the rate and pattern of interseismic deformation. We develop a simple analytic viscoelastic model of the surface velocity field through a clustered earthquake cycle by superposing the velocities of individual earthquake cycles of constant period but varying phase. Velocity profiles prior to and after an earthquake show a wider range of behavior than they do for earthquake cycles with constant repeat times. These new types of behavior provide possible explanations for discrepancies between geologic estimates of long-term fault slip rates and slip rate estimates from geodetic data. *INDEX TERMS:* 8123 Tectonophysics: Dynamics, seismotectonics; 8159 Tectonophysics: Rheology—crust and lithosphere; 8150 Tectonophysics: Plate boundary—general (3040). **Citation:** Meade, B. J., and B. H. Hager (2004), Viscoelastic deformation for a clustered earthquake cycle, *Geophys. Res. Lett.*, *31*, L10610, doi:10.1029/2004GL019643.

1. Introduction

[2] Characterizations of the temporal pattern of earthquakes range from periodic [e.g., *Reid*, 1910] to chaotic [e.g., *Scholz*, 1992]. Nearly periodic events have been recognized in the rupture history revealed by paleoseismic data in New Zealand [*Bull*, 1996]. Other ancient large earthquake catalogs reveal behavior that is clustered in time [e.g., *Wallace*, 1987; *Swan*, 1988; *Sieh et al.*, 1989; *Grant and Sieh*, 1994; *Marco et al.*, 1996; *Rockwell et al.*, 2000; *Weldon et al.*, 2002; *Friedrich et al.*, 2003]. A clustered earthquake cycle consists of a small number of earthquakes, typically 2–6, occurring in rapid succession on the same fault segment. This active period is followed by a quiet period devoid of major coseismic events (Figure 1). The time intervals reported for a single clustered earthquake cycle range widely, from several hundred years for the Carrizo segment of the San Andreas Fault [*Sieh et al.*, 1989], to 20,000–30,000 yrs for the Wasatch fault in eastern Utah [*Friederich et al.*, 2003], the Dead Sea fault [*Marco et al.*, 1996], and the Xiaojiang fault [*Xu and Deng*, 1996].

[3] Several theoretical investigations have addressed the possible causes of clustering. For example, *Ben-Zion et al.* [1999] and *Lyakhovsky et al.* [2001] showed that fault healing and damage rheology could lead to a response that alternates between active and quiescent periods. *Ben-Zion et al.* [1993] and *Lynch et al.* [2003] showed that time dependent strain rates in a viscoelastic substrate below the seismogenic zone could result in clustering. S. Kenner and M. Simons (Postseismic reloading: A source for temporal clustering of major earthquakes along individual fault segments, submitted to *Geophysical Journal International,* 2004, hereinafter referred to as Kenner and Simons, submitted manuscript, 2004) used a simple analog spring-dashpot-slider system to show that low viscosities and low loading rates tend to promote clustering. The question that we address here is how earthquake clustering influences the temporal variation in the velocity field near a fault. Our model provides a new framework for interpreting geodetic observations of interseismic deformation with time-dependent models that include information about the fault rupture history.

2. A Simple Clustered Earthquake Cycle

[4] Consider the simple clustered earthquake cycle (CEC) shown in Figure 1. Each CEC, of inter-cluster period T, consists of an active period, with n earthquakes offset by ΔT years, and a quiet period, of duration $T - \Delta T(n - 1)$. If s is the characteristic coseismic slip per event and v_0 is the long-term geologic slip rate of the fault (both assumed constant over a time long compared with T) the balance between coseismic slip and long-term geologic slip is given by $ns = v_0 T$. For the model shown in Figure 1, $n = 4$ and $\Delta T = T/10$. We also define the average recurrence interval, $T_{av} = T/n$, which gives the relation $s = v_0 T_{av}$.

[5] The temporal evolution of the surface velocity field during the earthquake cycle depends on the fault geometry and the rheology of the system. Here we consider the deformation associated with an infinitely long strike-slip fault in an elastic layer of thickness H overlying a half space consisting of a Maxwell viscoelastic material. *Savage and Prescott* [1978, hereinafter referred to as SP78] and *Savage* [2000] described the time evolution of the surface velocity field through an earthquake cycle for this model, assuming that earthquakes are strictly periodic with period, T. The resulting velocity field is a function of two additional times: the time since the last earthquake, t, and the Maxwell relaxation time of the viscoelastic halfspace, $\tau_M = \eta/\mu$, where μ is the shear modulus and η is the dynamic viscosity. Because of the wide range in T observed, it is useful to combine these three times into dimensionless parameters, only two of which are independent. Since we are investigating repeating earthquakes, we follow SP78 in using the dimensionless parameters $\tau_0 = T/2\tau_M$, and $t' = t/T$. For the CEC model, it is also useful to define a dimensionless active period interevent time $\Delta T' = \Delta T/T$.

[6] If we assume that the upper layer, except at the fault, is completely elastic and that the forcing is steady, the single and clustered earthquake cycles must balance interseismic

[1] Now at Department of Earth and Planetary Sciences, Harvard University, Cambridge, Massachusetts, USA.

0094-8276/04/2004GL019643$05.00

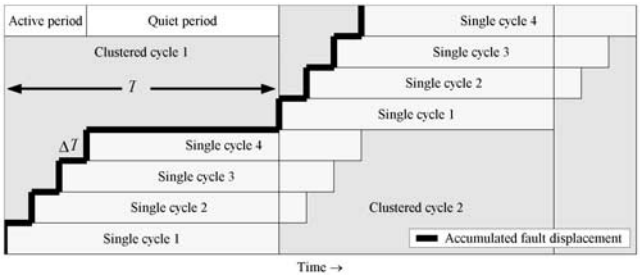

Figure 1. A schematic diagram of a simple clustered earthquake cycle (CEC). Each single earthquake cycle is represented by a thin gray rectangle. These are offset and stacked on top of each other to emphasize the overlapping nature of the earthquake cycles. The length of each earthquake cycle is the same as the CEC. The heavy dark line shows displacement history at the fault trace.

strain accumulation and coseismic strain release over long times. Our CEC model can be taken to the limit of a periodic earthquake model with long-term geologic slip rate in two ways. If n and s are held constant, with $\tau_0^{\text{periodic}} = \tau_0/n$, and period $\Delta T = T/n = T_{\text{av}}$, the model becomes identical to the periodic SP78 model. Alternatively, in the limit that ΔT goes to zero, the model becomes periodic with period T, but with the slip in the composite event increased proportionally, to ns, to balance the geologic rate. In comparing our results to those for periodic earthquakes, both limits are of interest and it is important to specify which is used.

[7] It is straightforward to generalize the SP78 model to the CEC shown in Figure 1. A CEC begins with the onset of one active period and ends at the start of the next. The CEC can be thought of as the superposition of n individual earthquake cycles, each with period T. For each of the individual earthquake cycles, τ_0 is defined in terms of T, not in terms of T_{av} for the entire cluster. The dimensionless fault-parallel surface velocity can be calculated by summing the contributions from the individual earthquake cycles:

$$v_C(t', \tau_0) = \sum_k v_S\left(\tau_0 t'_k, \tau_0\right) \tag{1}$$

where t'_k is the dimensionless time for each of the k contributing earthquake cycles, and v_S is the velocity from the SP78 model. Here, we model the behavior of a CEC with $n = 4$ earthquakes, each separated by $\Delta T' = 0.1$, and a relaxation parameter $\tau_0 = 5$. For example, for a choice of $T =$ 500 year ($\tau_0 = 5$ if $\eta \approx 5 \times 10^{19}$ Pa · s and $\mu = 30$ GPa), the active and quiet periods are 150 and 350 years long respectively. The average velocity profile for our viscoelastic model is given by $v = v_0\, \pi^{-1} \tan^{-1}(x/H)$, where x is the distance from the fault trace, H is the locking depth and v_0 is the slip rate. This profile, which is identical to that predicted for a steady state elastic model [e.g., *Savage and Burford*, 1973], provides a useful reference for examining the time-dependent effects of viscoelasticity.

[8] Figure 2 shows the fault-parallel velocity profiles at various times through a CEC. For reference, we show the results for the two limiting cases of periodic earthquakes - the case $\Delta T' = 0$, with slip $4s$ (Figure 2a) and the case $\Delta T' =$ 1/4 with slip s (Figure 2b). For large τ_0, (e.g., $\tau_0 = 5$, Figure 2a) there are large variations through the earthquake cycle. Immediately after an earthquake, the fault-parallel velocity is greater than the average velocity and peaks at a distance $x/H = 2$ from the fault trace. Late in the cycle, as the next earthquake approaches, the surface velocities decay to values lower than the average and the maximum velocity is found far away from the fault. This pattern can be described as "slow before, fast after". In Figure 2b, the recurrence interval is a factor of 4 smaller than that in Figure 2a, and the effective τ_0 is a factor of 4 smaller, $\tau_0 =$ 5/4. The model in Figure 2a can be viewed as having the same geologic slip rate with larger, less frequent

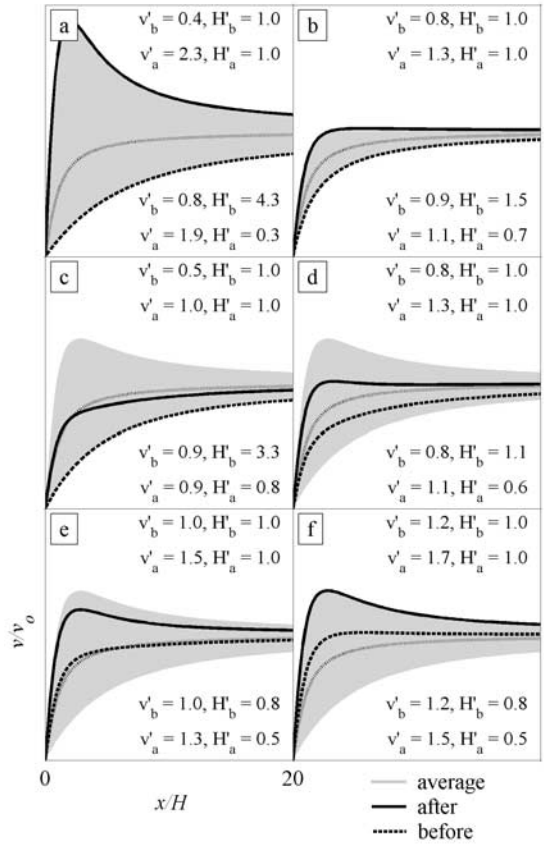

Figure 2. Interseismic velocity profiles. Each figure shows half of a fault parallel velocity profile at various times through the earthquake cycle. In all cases, the finely dashed line is the average profile, the solid black line is the profile immediately following an event and the coarsely dashed line shows the velocity profile immediately prior to the event. The gray shaded regions indicate the full range of velocity profiles through the CEC. The axes are the same for all Figures but are shown on only the lower left figure for clarity. a) Profiles for a single earthquake cycle with τ_0^{ref}. b) Profiles for a single earthquake cycle with $\tau_0^{\text{ref}}/4$. c) Profiles for the first event in a CEC with τ_0^{ref}. d) Profiles for the second event in a CEC with τ_0^{ref}. e) Profiles for the third event in a CEC with τ_0^{ref}. f) Profiles for the fourth, and last, event in a CEC with τ_0^{ref}. The normalized estimated slip rates, v', and locking depths, H', are from best-fit steady state models. The subscripts a and b indicate the after and before profiles respectively. In each panel the upper set of values are for the case where the locking depth is fixed at its true value. For the lower set of numbers the locking depth is estimated simultaneously with the slip rate.

earthquakes than the model in Figure 2b. Lower effective values of τ_0, (Figure 2b) yield less variation through the earthquake cycle.

[9] Immediately after the first earthquake in the CEC, the velocity is slower than the reference steady state elastic half space profile (Figure 2c). This is because the three other out of phase earthquake sequences are late in their cycles and effectively reduce the total velocity. This "slow before, slow after" behavior is different from the single period model where the velocity following an earthquake is always greater than the reference value (Figures 2a and 2b).

[10] After additional active period earthquakes (Figure 2d), the pre-event velocity is "slow" and the postseismic is "fast", just as in the single period model. Late in the active period the pre-event velocity may be greater than the average due to the influence of the high velocities generated by the previous earthquakes ("fast before, fast after", Figure 2f). Again, this is different from the prediction for a single period earthquake cycle, where the velocity preceding an earthquake is always less then the reference value. Of course, at the end of the quiet period, all velocities are much lower than the average value, as all of the earthquakes are late in their cycles. In sum, the pattern of deformation immediately before and after earthquakes in the presence of clustering shows a range of behavior including "slow before, slow after" for the first event in the sequence, "slow before, fast after" for the second, and "fast before, fast after" for the fourth. The interseismic velocity profiles between the third and fourth events in the active period are remarkably similar to reference profiles for a shallower locking depth and a slightly lower slip rate.

[11] If the time-dependent effects of viscoelastic relaxation through the earthquake cycle are ignored, deviations from the average may be mapped into an elastic halfspace model as fast/slow slip rates or shallow/deep locking depths. We quantify this mapping by estimating the apparent elastic parameters for the velocity profiles in Figure 2. For each before/after profile we use the elastic halfspace model to estimate the normalized slip rate, $v' = v_{est}/v_{true}$. We consider cases where the normalized locking depth, $H' = H_{est}/H_{true}$, is known *a priori*, and cases where it is estimated simultaneously with the slip rate. For the cases presented here we use only the portion of the velocity profile within $x/H = 5$ of the fault to simulate a typical distribution of observations.

[12] With a fixed locking depth, the slip rate estimates before/after a periodic earthquake ($\tau_0 = 5$, Figure 2a) are approximately a factor of two larger/smaller than the true values for the early/late velocity profiles respectively. Through our example CEC, the slip rate variation ranges from a low of $v' = 0.5$ prior to the first event in the active period to a high of $v' = 1.5$ after the last event. The variation in estimated slip rate is 10–50% smaller when the locking depth is estimated simultaneously. Shallow/deep locking depths correspond to the early/late profiles respectively for perfectly periodic earthquakes. The same is true for profiles within a clustered earthquake cycle, with the exception of the profiles prior to events in the later half of the active period (Figures 2e and 2f). Here H' is less than unity due to the influence of multiple earthquakes that are early in their individual cycles.

3. Discussion

[13] The parameter τ_0 can be shown to be the same as the parameter that *Kenner and Simons* (submitted manuscript, 2004) name the Wallace Number and use to characterize their models; systems with large τ_0 tended to show clustered earthquakes. Fault slip rates can be estimated by fitting observed velocities to interseismic deformation models. This mapping allows us to compare geodetic slip rates with long-term slip rates obtained with paleoseismic and geomorphic methods.

[14] *Friederich et al.* [2003] found that although tectonic rates on the Wasatch fault are approximately constant when averaged over 10^6 years, a cluster of ~5 events during the past 9 ka following a 30 ka quiescent period demonstrates substantial variability over 10^4 year time scales. They speculated that, in the absence of short-term postseismic transients, the geodetic rate should be comparable to the long-term geologic average. In contrast, the observed geodetic rate is higher than the long-term geodetic rate, as our model predicts late in an active period (Figure 2f). Unfortunately our ability to use this discrepancy to quantitatively constrain rheologic parameters is limited because the relationship between the geologically determined vertical rates and the geodetically estimated horizontal rates is highly sensitive to the poorly constrained fault geometry.

[15] The Eastern California Shear Zone is another example where geodetic and geologic observations may be more readily interpreted with a clustered rather than periodic earthquake cycle model. Geodetic estimates of slip rates on the strike slip faults south of the Garlock fault [*McClusky et al.*, 2001; *Peltzer et al.*, 2001] tend to be higher than geologic estimates [e.g., *Rockwell et al.*, 2000; *Oskin and Iriondo*, 2004] by at least a factor of two. Both *McClusky et al.* [2001] and *Peltzer et al.* [2001] determined slip rates after the 1992 Landers earthquake that are consistent with the high strain rate estimated prior to the event [*Sauber et al.*, 1994]. Fast rates both before and after the Landers earthquake are incompatible with the variation in surface deformation predicted by the single period earthquake cycle model. However, the CEC model does show this "fast before, fast after" behavior late in the active period (Figure 2f). To double the apparent slip rate prior to the last earthquake in the cycle in the scenario we investigate would require $\tau_0 >= 5$. This would be reasonable for the ECSZ, where the low geologic slip rates indicate that the average repeat time is quite long [e.g., *Rockwell et al.*, 2000].

[16] The pre-earthquake velocity profile in Figure 2f is similar to the profile that would be expected from the same fault slip rate but with a shallow locking depth. *Peltzer et al.* [2001] estimated a shallow locking depth for the Blackwater fault in California's Mojave Desert using radar interferometry. An alternative explanation is that the fault is not locked to a shallow depth, but is instead late in an active period of a CEC.

4. Conclusions

[17] A viscoelastic clustered earthquake cycle model shows a wider variety of pre- and post-seismic behavior

than does the single-period earthquake cycle model due to the overlapping of viscoelastic relaxation effects from several relatively recent earthquakes. This model highlights the challenge of interpreting geodetic measurements of crustal deformation in the context of viscoelastic relaxation. The CEC model provides both the motivation and a mechanism for integrating paleoseismic rupture histories with present day estimates of interseismic surface velocities to determine the dynamics of actively deforming zones. This model may reconcile apparent differences between short and long-term fault slip rates as well as provide an alternative explanation for estimates of apparently shallow fault locking depths.

[18] **Acknowledgments.** This research was supported by the Southern California Earthquake Center. SCEC is funded by NSF Cooperative Agreement EAR-0106924 and USGS Cooperative Agreement 02HQAG0008. The SCEC contribution number for this paper is 769. We thank Anke Friedrich for helpful discussions regarding the Wasatch fault and Roland Bürgmann and Yehuda Ben-Zion for thoughtful reviews.

References

Ben-Zion, Y., J. R. Rice, and R. Dmowska (1993), Interaction of the San Andreas fault creeping segment with adjacent great rupture zones, and earthquake recurrence at Parkfield, *J. Geophys. Res.*, *98*, 2135–2144.

Ben-Zion, Y., K. Dahmen, V. Lyakhovsky, D. Ertas, and A. Agnon (1999), Self-driven mode switching of earthquake activity on a fault system, *Earth Planet. Sci. Lett.*, *172*, 11–21.

Bull, B. W. (1996), Prehistorical earthquakes on the Alpine fault, New Zealand, *J. Geophys. Res.*, *101*, 6037–6050.

Friedrich, A. M., B. P. Wernicke, N. Niemi, R. A. Bennett, and J. L. Davis (2003), Comparison of geodetic and geologic data from the Wasatch region, Utah, and implications for the spectral character of Earth deformation at periods of 10 to 10 million years, *J. Geophys. Res.*, *108*(B4), 2199, doi:10.1029/2001JB000682.

Grant, L. B., and K. Sieh (1994), Paleoseismic evidence of clustered earthquakes on the San Andreas fault in the Carrizo Plain, California, *J. Geophys. Res.*, *99*, 6819–6841.

Lyakhovsky, V., Y. Ben-Zion, and A. Agnon (2001), Earthquake cycle, fault zones, and seismicity patterns in a rheologically layered lithosphere, *J. Geophys. Res.*, *106*, 4103–4120.

Lynch, J. C., R. Bürgmann, M. A. Richards, and R. M. Ferencz (2003), When faults communicate: Viscoelastic coupling and earthquake clustering in a simple two-fault strike-slip system, *Geophys. Res. Lett.*, *30*(6), 1270, doi:10.1029/2002GL016765.

Marco, S., M. Stein, and A. Agnon (1996), Long-term earthquake clustering: A 50,000-year paleoseismic record in the Dead Sea Graben, *J. Geophys. Res.*, *106*, 4103–4120.

McClusky, S. C., S. C. Bjornstad, B. H. Hager, R. W. King, B. J. Meade, M. M. Miller, F. C. Monastero, and B. J. Souter (2001), Present-day kinematics of the Eastern California Shear Zone from a geodetically constrained block model, *Geophys. Res. Lett.*, *28*, 3339–3372.

Oskin, M., and A. Iriondo (2004), Large magnitude transient strain accumulation on the Blackwater fault, Eastern California Shear Zone, *Geology*, *32*, 313–316.

Peltzer, G., F. Crampe, S. Hensley, and P. Rosen (2001), Transient strain accumulation and fault interaction in the Eastern California Shear Zone, *Geology*, *29*, 975–978.

Reid, H. F. (1910), *The California Earthquake of April 18, 1906: Report of the State Earthquake Investigation Commission*, vol. 2, *The Mechanics of the Earthquake*, 192 pp., Carnegie Inst. of Wash., Washington, D. C.

Rockwell, T. K., S. Lindvall, M. Herzberg, D. Murback, T. Dawson, and G. Berger (2000), Paleoseismology of the Johnson Valley, Kickapoo, and Homestead Valley faults: Clustering of earthquakes in the Eastern California Shear Zone, *Bull. Seismol. Soc. Am.*, *90*, 1200–1236.

Sauber, J., W. Thatcher, S. C. Solomon, and M. Lisowski (1994), Geodetic slip rate for the Eastern California Shear Zone and the recurrence time of Mojave Desert earthquakes, *Nature*, *367*, 264–266.

Savage, J. C. (2000), Viscoelastic coupling model for the earthquake cycle driven from below, *J. Geophys. Res.*, *105*, 25,525–25,532.

Savage, J. C., and R. O. Burford (1973), Geodetic determination of the relative plate motion in central California, *J. Geophys. Res.*, *78*, 832–845.

Savage, J. C., and W. H. Prescott (1978), Asthenosphere readjustment and the earthquake cycle, *J. Geophys. Res.*, *78*, 3369–3376.

Scholz, C. H. (1992), Earthquake predictions: Models of the seismic cycle, *Nature*, *335*, 774–775.

Sieh, K., M. Stuiver, and D. Brillinger (1989), A more precise chronology of earthquakes produced by the San Andreas fault in Southern California, *J. Geophys. Res.*, *94*, 603–623.

Swan, F. H. (1988), Temporal clustering of paleoseismic events on the Oued Fodda fault, Algeria, *Geology*, *16*, 1092–1095.

Wallace, R. E. (1987), Grouping and migration of surface faulting and variation in slip rtes on faults in the Great Basin province, *Bull. Seismol. Soc. Am.*, *77*, 868–877.

Weldon, R. J., T. E. Fumal, T. J. Powers, S. K. Pezzopane, K. M. Scharer, and J. C. Hamilton (2002), Structure and earthquake offsets on the San Andreas fault at the Wrightwood, California, paleoseismic site, *Bull. Seismol. Soc. Am.*, *92*, 2704–2725.

Xu, X., and Q. Deng (1996), Nonlinear characteristics of paleoseismicity in China, *J. Geophys. Res.*, *101*, 6209–6231.

B. H. Hager, Department of Earth, Atmospheric and Planetary Sciences, Massachusetts Institute of Technology, Cambridge, MA 02139, USA.

B. J. Meade, Department of Earth and Planetary Sciences, Harvard University, Cambridge, MA 02138, USA. (meade@rupture.harvard.edu)